

---

# Cathedral Ceilings: A Test Building Evaluation in a Cool, Humid Climate

**Hugo Hens, Ph.D.**  
Member ASHRAE

**Arnold Janssens, Ph.D.**  
Member ASHRAE

## ABSTRACT

*This paper describes a series of field tests on four types of cathedral ceilings with six different designs. During the two years of testing, airtightness, wind washing, thermal performance, and moisture were monitored. The outside environment at the test site was representative of a cool, humid climate. Indoors, a normally heated, moderately humid environment was maintained. The test results show that airtightness and wind washing are the main elements fixing hygrothermal response. The tests nevertheless confirm that a compact cathedral ceiling, with a windtight but vapor permeable underlay, no airspace above the thermal insulation and an effective airflow retarder below, is the best choice in a cool, humid climate.*

---

## INTRODUCTION

In Western European homes, attics have become part of the living space. Therefore, the thermal insulation was moved from the ceiling to the pitches, giving birth to the cathedral ceiling. In the 1970s and 1980s, many cathedral ceilings failed prematurely because of condensation problems (see Figure 1) (Anon. 1975-2000). The measures the roof industry advanced to avoid the problem were to (1) include a ventilated airspace between the thermal insulation and the underlay and (2) add a vapor retarder on the inside (Anon. 1989). The ventilation between the thermal insulation and the underlay was thought to be particularly important.

In the late 1980s, Künzle and Großkinsky (1989) proved experimentally that the beneficial effect of ventilation is completely uncertain as long as airtightness of the pitches is not guaranteed. During the same period, a series of hot box tests on various cathedral ceilings and field tests on 20 different roof designs underlined that not only the hygric but also the thermal performance was jeopardized if airtightness was not secured (Janssens et al. 1992, 1999; Hens and Janssens 1999). Derome added evidence to the statement that airtightness and not ventilation should be a prime concern. In a series of large climate chamber tests on roofs that were insulated with blown

cellulose fiber, she demonstrated that most condensation developed in the section with the highest air permeance (Derome 1998). In the U.S., Rose (2001) tested different cathedral ceilings with various designs. One of the concerns was shingle temperature. He found that the beneficial effect of ventilation on shingle temperature was marginal. A last fact that gradually countered the ventilation requirement was the larger insulation thicknesses of the nineties that building regulations imposed with the Kyoto protocol in mind. These substantially increased the costs of leaving an airspace between the insulation and the underlay. Compact roof designs, with the underlay directly on the insulation, were cheaper and, as field tests showed, very moisture tolerant if sufficiently airtight (Hens and Janssens 1999). Some manufacturers substantiated that advantage by promoting the usage of a vapor-permeable underlay (Künzel and Großkinsky 1992; Ojanen 2001). The statement, however, that a vapor-permeable underlay may compensate for failing airtightness was disputable, as field tests showed. Also, smart vapor retarders and diode vapor retarders were advocated as solutions by some research institutes and manufacturers (Sedlbauer and Künzle 2000).

The confusion created by all of these messages (ventilation not necessary, compact better than ventilated, ventilation

---

**Hugo Hens** is a professor in the Department of Civil Engineering, Laboratory of Building Physics, K.U. Leuven, Belgium. **Arnold Janssens** is a professor of building physics in the Department of Architecture and Urban Design, Universiteit Gent, Belgium.

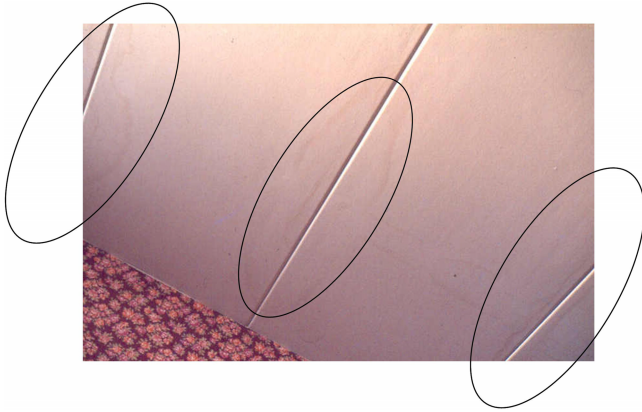


**Figure 1** *Traces of dripping moisture on the internal lining of a sleeping room. The cause of the dripping is interstitial condensation in the cathedral ceiling.*

nevertheless needed, airtightness essential, vapor-permeable underlay compensating for insufficient airtightness, smart vapor retarder a solution for all problems, etc.) was a convincing argument to start a two-year field testing program on four types of double-pitch cathedral ceilings, covered with tiles or fiber-cement corrugated plates. For types 1 and 2, two different designs were considered. The six designs had one performance requirement in common: an SI whole roof thermal transmittance  $\leq 0.2 \text{ W}/(\text{m}^2\cdot\text{K})$  should be achieved. They, however, were quite different on several points: (1) site-constructed roofs versus roofs constructed with prefabricated pitch elements, (2) the use of an insulated under-roof versus the use of a non-insulating underlay, (3) ventilation between insulation and underlay versus compact pitch, (4) additional airflow retarder underneath the insulation versus no additional airflow retarder, and (5) the use of a vapor-permeable underlay versus the use of a vapor-retarding underlay (Janssens et al. 1995; Janssens and Hens 1998, 1999).

## TEST BUILDING AND CATHEDRAL CEILING TYPES AND DESIGNS

### Test Building

The building used for the field tests was specially designed to develop and evaluate energy-efficient and durable envelopes and roof designs (Janssens et al. 1995). It was conceived as a rectangular structure with a pitched roof module, a flat roof module and the HVAC room, the data room, and a small module for advanced envelope testing in between. The building allows testing of 20 envelope and roof designs exposed to the cool and humid Western European climate. Half of the wall and roof surfaces look southwest, half northeast. In Western Europe, southwest is the prevailing wind, wind-driven rain, and solar irradiation direction, while northeast hardly receives any sun and rain. Each of the pitches that



**Figure 2** *The test building.*

contain the cathedral ceilings is 3.6 m long in horizontal projection (total span 7.2 m). Their slope is  $45^\circ$ . Each of the six cathedral ceiling elements has a width of 1.8 m (Figure 2).

In the test building, residential as well as very humid conditions can be imposed. This is realized by an air-conditioning system with local steam humidifiers and a temperature and relative humidity control. Air pressure differences between the inside and the outside are managed through ventilation grids in the entrance doors, the leaks in the different roof and wall elements, and fans in the HVAC system. The building has its own weather station 1 m above the ridge that registers all outside climate parameters on a one minute basis and calculates the averages every ten minutes. Also, the inside temperature and relative humidity are monitored every ten minutes.

### The Test Roofs

The four types of cathedral ceiling proposed for testing by the participating manufacturers are shown in Figure 3. The four types include the following six different designs:

1. **Type 1 (two designs).** A compact cathedral ceiling with 19 cm of glass-wool insulation. Sections (from the outside to the inside): (1) concrete tiles, (2) vapor-permeable underlay with overlapping joints (vapor permeance =  $9.3 \cdot 10^{-9} \text{ s/m}$ ), (3) 14 cm of glass-wool between the rafters ( $\rho = 18 \text{ kg/m}^3$ ,  $\lambda_{10} = 0.034 \text{ W}/[\text{m}\cdot\text{K}]$ ), (4) 5 cm of glass-wool between the horizontal laths that are nailed against the rafters ( $\lambda_{10} = 0.040 \text{ W}/\text{m}\cdot\text{K}$ ), and (5) an inside lining of gypsum board, painted at the underside (vapor permeance  $5.3 \cdot 10^{-11} \text{ s/m}$ ). In design 1 a polyethylene airflow retarder separates the 14-cm-thick glass-wool layer from the 5-cm-thick glass-wool layer (vapor permeance  $3.1 \cdot 10^{-12} \text{ s/m}$ ). Design 2 does not have that airflow retarder.
2. **Type 2 (two designs).** A ventilated cathedral ceiling with 19 cm of glass-wool insulation. The designs differ on two points from type 1: (1) the underlay consists of a bituminous felt (vapor permeance:  $4.6 \cdot 10^{-10} \text{ s/m}$ ), and (2) a 5-cm-thick ventilated airspace is included between the insulation and

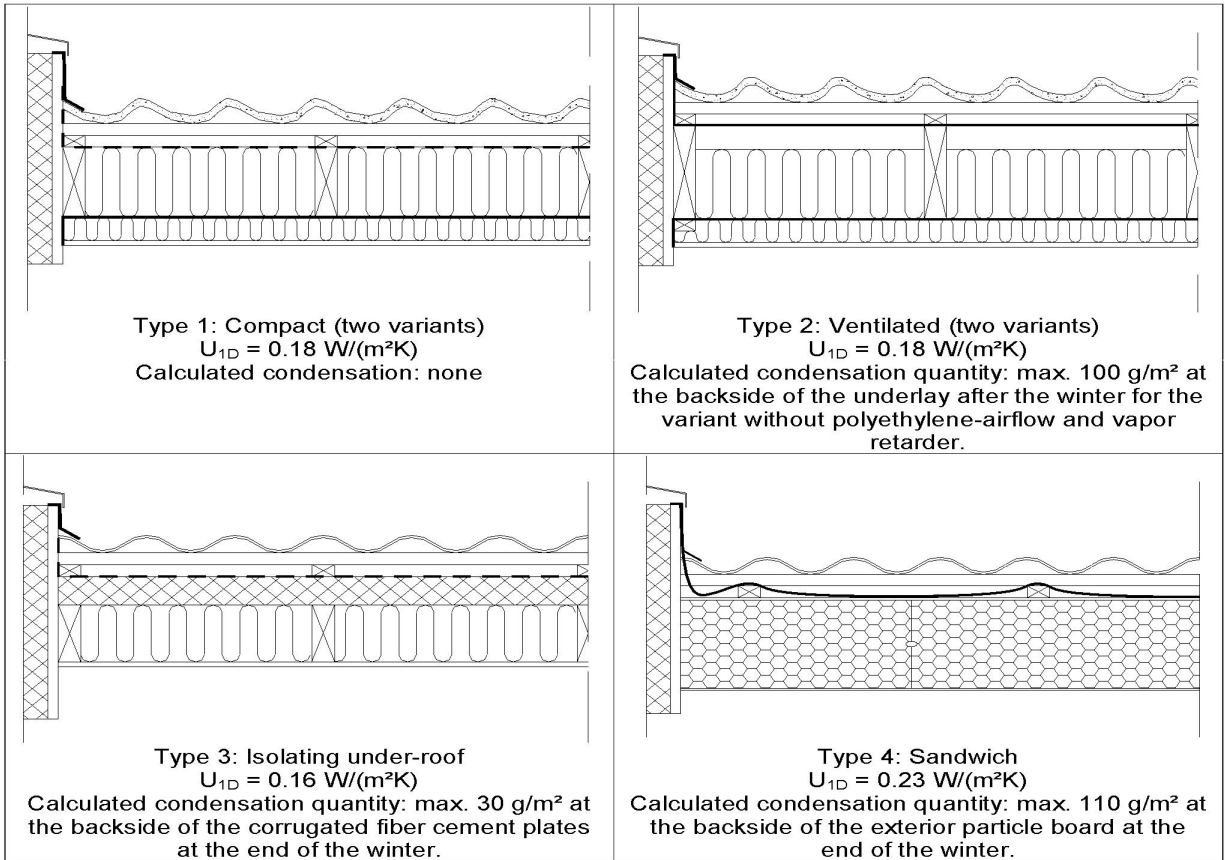


**Figure 3** Cathedral ceiling types and projected performances.

the underlay. That space has an air inlet at the eaves and an air outlet at the ridge. Also in design 1, a polyethylene airflow retarder separates the 14-cm-thick glass-wool layer from the 5-cm-thick glass-wool layer (vapor permeance  $3.1 \cdot 10^{-12} \text{ s}/\text{m}$ ). Design 2 does not have that airflow and vapor retarder.

- Type 3.** A cathedral ceiling with 12 cm of glass-wool insulation and a 6-cm-thick XPS under-roof. Roof sections (from the outside to the inside): (1) corrugated fiber cement plates, (2) 6-cm-thick XPS-under-roof with nut and feeder closure between the boards ( $\lambda_{10} = 0.026 \text{ W}/[\text{m}/\text{K}]$ ) that is screwed on the rafters and covered with a vapor-permeable underlay (vapor permeance:  $9.3 \cdot 10^{-9} \text{ s}/\text{m}$ ), (3) 12 cm of glass-wool insulation between the rafters ( $\lambda_{10} = 0.034 \text{ W}/\text{m}/\text{K}$ ), and (4) an inside lining of gypsum board, painted at the underside (vapor permeance  $5.3 \cdot 10^{-11} \text{ s}/\text{m}$ ).
- Type 4.** Cathedral ceiling composed of prefabricated sandwich elements. Roof sections (from the outside to the inside): (1) corrugated fiber cement plates, (2) micro-perforated plastic foil with overlapping lanes (vapor permeance  $1.2 \cdot 10^{-10} \text{ s}/\text{m}$ ), and (3) 20-cm-thick sandwich elements composed of  $2 \times 4 \text{ mm}$  particle board (vapor permeance  $1.9 \cdot 10^{-10} \text{ s}/\text{m}$ ) with 19 cm EPS in between ( $\lambda_{10} = 0.048 \text{ W}/[\text{m}/\text{K}]$ ).

In all six designs, airtightness got specific attention. Perforations, if any, in the inside lining were carefully sealed and all joints between the gypsum boards, between the gypsum boards and the walls, and between the gypsum boards and the rafters that separated the different roof designs were first taped, then finished with a joint filler and additionally sealed with silicone.

Figure 3 gives the clear roof thermal transmittance ( $U$ ) as intended (calculated in accordance to the Belgian standard B62-002 [IBN-BIN 1987]) and the condensation rate that could be expected if calculated according to the Glaser methodology, using the sol-air temperature for condensation as explained in Anon (1982). All designs, except type 4, had an intended thermal transmittance that satisfied the  $0.2 \text{ W}/(\text{m}^2\text{K})$  requirement. Type 4 failed because the EPS in the sandwich panel had too low a density. The condensation rates given in the figure also did not pose any durability risk. Five of the six cathedral ceilings apparently deserved the classification “well designed and moisture tolerant.” Type 4 just required a heavier EPS (EPS20 instead of EPS10).

At 1, 2.54, and 4.09 m from the eaves, the six cathedral ceiling designs were equipped with thermocouples in all interfaces between layers and with air tubes, plus relative humidity

sensors below the underlay. Condensation sensors were fixed at the backside of the underlay in the type 1 and 2 designs, 1 and 4.09 m from the eaves. At mid span, a heat flow meter was taped against the gypsum board. All temperatures, the heat flow rate, the relative humidity below the underlay, the

condensation signals, and the inside and outside climate were logged continuously, averaged on a ten minute basis and stored on hard disk.

### Performances Evaluated by Measurement

Table 1 lists the performances that were evaluated. The set of performances in the table is taken from the Annex 32, "Array of Envelope Performances," as explained in Hendriks and Hens (2000).

**Table 1. Performances Tested According to the International Energy Agency, Executive Committee on Energy Conservation in Buildings and Community Systems Annex 32 Array of Envelope Performances (Hendriks et al. 2000)**

Topic	Performances
Heat and mass	Airtightness <ul style="list-style-type: none"> <li>• Air permeance</li> <li>• Ventilation and wind washing</li> <li>• Buoyancy flow around the fill</li> </ul>
	Thermal insulation <ul style="list-style-type: none"> <li>• Clear and whole roof U-factor</li> </ul>
	Moisture response <ul style="list-style-type: none"> <li>• Interstitial condensation</li> </ul>
Service life	Biological attack (mold)

## EXPERIMENTAL RESULTS

### Exterior and Interior Climate

Figure 4 summarizes daily average outside climatic data, measured at the test building site: air temperature, relative humidity, solar irradiation on a horizontal surface, and wind-driven rain in the middle of the southwest facade. The values are typical for the cool, wet climate of Western Europe: moderate winter temperatures with some lonely cold spells, moderate summer temperatures, high relative humidity, little solar irradiation in winter, and some wind-driven rain.

In the test building, an inside climate class 3 situation was maintained during the winter, with an average air temperature

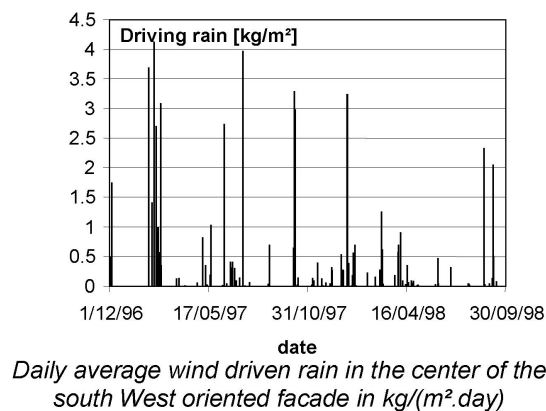
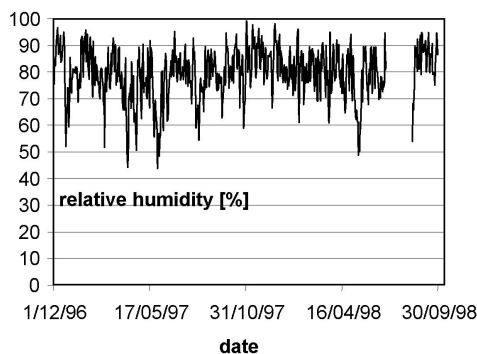
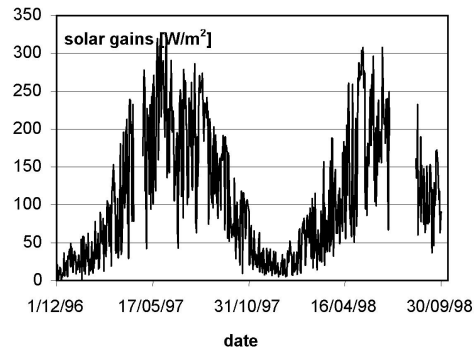
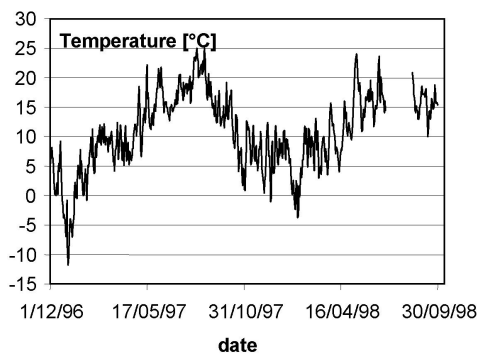


Figure 4 Outside climate during the test period.

of 21°C and an average inside vapor pressure excess of 600 Pa. Inside climate class 3 is representative for the inside vapor pressure excess measured in small dwellings, which, in Western European countries, are built under the common denominator of “subsidized housing” (Sanders 1996).

### Airtightness

The airtightness and the airflow patterns in the cathedral ceilings were analyzed using an SF<sub>6</sub> tracer. To get the data, the tracer was first injected in the test building to maintain a constant concentration, and the concentration built up in the ceilings was logged. Then the airflow patterns were mapped by injecting the tracer at a constant flow in a point in the cathedral ceilings and by simultaneously measuring concentration built up in all other points in the ceilings where air tubes were present. Both methods give qualitative results. The data gained allowed a fair estimate of the airtightness, using a model that considers the cathedral ceiling as a volume that is homogeneously filled with an air/tracer mixture. If the roof volume is small enough to neglect damping and time lag, then applying conservation of mass gives

$$C(t) = \frac{G_{ex}}{G_{ex} + G_{in}(t)} C_1 \quad (1)$$

with  $G_{ex} = K_a \Delta p_a A$  and  $G_{in}(t) = n(t)V$ ,

where  $C(t)$  is the tracer concentration in the cathedral ceiling at time  $t$  (mg/m<sup>3</sup>),  $C_1$  is the constant tracer concentration in the building (mg/m<sup>3</sup>),  $G_{ex}$  is the air infiltration from the building into the cathedral ceiling (m<sup>3</sup>/s),  $G_{in}$  is the airflow from outside into the cathedral ceiling (m<sup>3</sup>/s),  $K_a$  is the air permeance of the cathedral ceiling (assumed to be a constant, kg/[m<sup>2</sup>·s·Pa]),  $\Delta P_a$

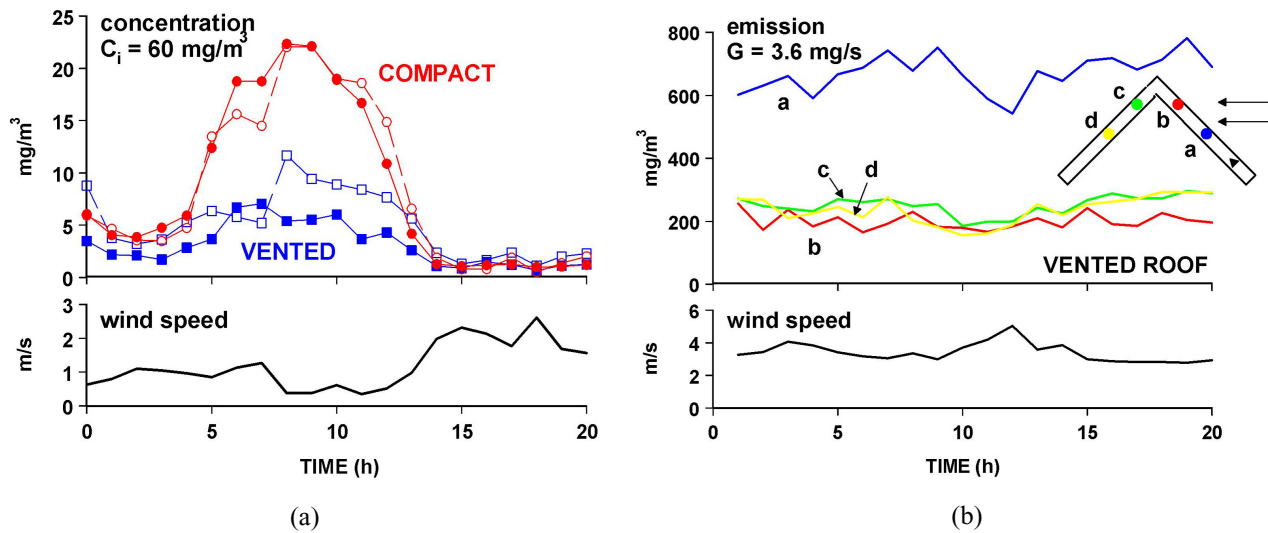
is the air overpressure in the building (7 Pa),  $A$  is the area of the pitch (m<sup>2</sup>),  $V$  is the roof volume between airflow retarder and underlay (m<sup>3</sup>), and  $n$  is the ventilation rate (s<sup>-1</sup>). The relationship between the airflow from outside and the wind velocity was determined by using the second series of measurements. These allowed us to calculate the airflow and to relate the values found to the measured wind velocity, using a least-squares linear approach. The result is

$$G_{in} = \frac{G_{tracer}}{C}, \quad G_{in} = a[v(t)] = 6 \cdot 10^{-6} v(t), \quad (2)$$

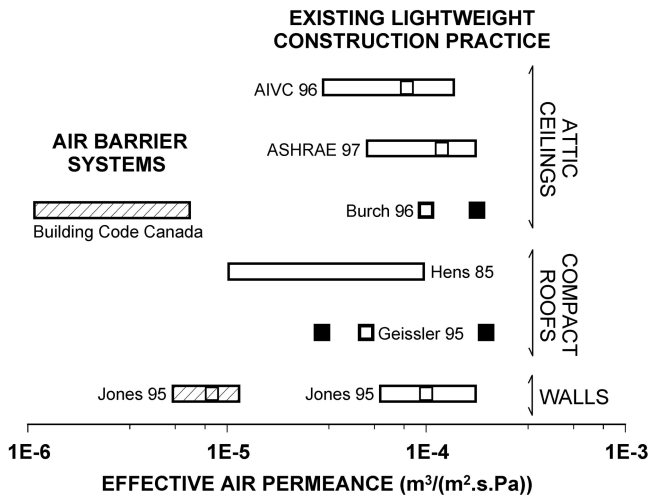
where  $G_{tracer}$  is the tracer flow rate (mg/s) and  $C$  is the average concentration in the cathedral ceiling (mg/m<sup>3</sup>).

Figure 5a gives the results of the first test for the type 1 and 2 cathedral ceilings. The tracer concentration in the building was 60 mg/m<sup>3</sup>. The measured concentration in the ceilings follows from two intermixing flows, an outside airflow with concentration zero and an inside airflow with concentration 60 mg/m<sup>3</sup>. The fact that a concentration different from zero is measured in the four designs proves that perfect airtightness was not achieved. Simultaneously, the low concentrations and the strong relationship with wind shows that outside air infiltration is smaller in the compact cathedral ceilings than it is in the ventilated cathedral ceilings. The results also show that adding a polyethylene airflow retarder creates hardly any benefit. This is due to the excellent airtightness of the painted gypsum board and the way the polyethylene was stapled against the rafters.

Figure 5b gives some results of the second test. The gas was dosed at the eave of the windward pitch. Outside air clearly infiltrates into the cathedral ceiling space through the



**Figure 5** (a) Test 1, tracer concentration in the roofs (constant tracer concentration in the building), and (b) Test 2, tracer injected at the windward eave, tracer concentration measured at three different positions in the roof space.



**Figure 6** Air permeance: comparison between the values measured on the test roofs, the values measured on roofs that simulate building practice, and the requirements, as given in the Canadian building code.

overlaps between the underlay lanes. The concentration in fact diminishes from mid-position to the ridge. The air at the leeward side in turn comes from the windward side. These results, which were noted in all cathedral ceilings except type 4, prove wind-washing to be present.

The data for the ventilated cathedral ceilings were used to quantify the area-averaged air permeance  $K_a$  of both the compact and the ventilated types (in  $\text{kg}/[\text{m}^2 \cdot \text{s} \cdot \text{Pa}]$ ). For that purpose,  $K_a$  was assumed to be a constant, the average 7 Pa air pressure excess in the building was taken as invariable, and the linear relationship given in Equation 2 between wind velocity and ventilation flow was used. Results: (1)  $K_a = 7.2 \cdot 10^{-6} \text{ kg}/(\text{m}^2 \cdot \text{s} \cdot \text{Pa})$  for the compact and ventilated cathedral ceilings with painted gypsum board lining, (2)  $K_a = 3.4 \cdot 10^{-6} \text{ kg}/(\text{m}^2 \cdot \text{s} \cdot \text{Pa})$  for the compact and ventilated cathedral ceiling with painted board gypsum lining and an additional polyethylene airflow retarder. When these results are compared with the air permeances, measured in practice or measured on roof pitches that include the imperfections seen in practice, then the four cathedral ceiling designs of types 1 and 2 may be accepted as very airtight (see Figure 6). A value of  $3.4 \cdot 10^{-6}$  and  $7.2 \cdot 10^{-6} \text{ kg}/(\text{m}^2 \cdot \text{s} \cdot \text{Pa})$  also fulfills the requirement that the air permeance coefficient should be lower than  $1 \cdot 10^{-5} \text{ kg}/(\text{m}^2 \cdot \text{s} \cdot \text{Pa}^b)$  if problematic interstitial condensation caused by air exfiltration should be avoided (the air permeance coefficient [symbol a] is related to the air permeance  $K_a$  by  $K_a = a(\Delta P_a)^{b-1}$ ) (Hens et al. 2003).

## Clear and Whole Roof Thermal Transmittance ( $U$ )

The effective thermal resistance ( $R_M$ ) of the four cathedral ceiling types was calculated by dividing the average heat flow rate measured on the inside surface over a given period of time by the average temperature difference between the inside surface and the upper surface of the thermal insulation over the same period of time (ASTM 1998). The maximum error in the effective thermal resistance defined this way was  $0.2 \text{ m}^2\text{K}/\text{W}$ . The clear roof thermal transmittance ( $U$ ) was then calculated as

$$U_M = \left( R_M + \frac{1}{h_i} + \frac{1}{h_e} \right)^{-1} \quad (\text{W}/(\text{m}^2\text{K})), \quad (3)$$

where  $h_i$  is the standardized surface film coefficient at the inside and  $h_e$  is the equivalent surface film coefficient at the upper surface of the insulation, taking into account the wind washing underneath the underlay and/or roof cover. Both were set equal to  $8 \text{ W}/(\text{m}^2\text{K})$ .

Table 2 gives the results for the six designs. For four designs, only the values at mid-span are given. To get a picture of possible scatter over the pitch, two cathedral ceilings got additional heat flow meters—one at 1 m from the eaves and the other at 1 m from the ridge. For these two ceilings, the three results are given. Values that deviate more from the intended clear roof U-factor than the measuring accuracy allows are printed in bold. Such values are found in the compact and the ventilated cathedral ceiling types 1 and 2, although only on the southwest pitch. The U-factors, measured locally, are systematically higher than the intended value in the ventilated type without polyethylene foil, even with an excess of 55%. The results further show that the local U-factors vary considerably over the length of the pitch, and although locally measured values are not always representative for the whole surface.

A further analysis showed that the thermal performance of the compact and the ventilated cathedral ceiling types 1 and 2, measured on a daily basis, varied with the daily mean wind velocity. To allow a clear distinction between wind impact and other factors that influenced the U-factor, the results were reassessed, using the thermal resistance measured during a windless day as a reference, and calling the ratio between the thermal resistance measured during a random day with wind velocity  $v$  and the reference the Nusselt number for the case considered.

$$\text{Nu}(v) = \frac{R_o}{R_M(v)} \quad (4)$$

A day was called windless when the mean wind velocity was below  $0.5 \text{ m/s}$  ( $R_o = R_M[v \leq 0.5 \text{ m/s}]$ ). The Nusselt number defined that way quantified the change in heat loss through the cathedral ceiling as a consequence of wind washing. If above 1, wind washing increases the loss. If below 1, wind washing diminishes the loss. Figure 7 shows a typical relationship between the measured daily mean Nusselt number and the daily wind velocity vector along the pitch—positive if directed from eave to pitch, negative if directed the other way around.

**Table 2. Measured Clear Roof Thermal Transmissivities ( $U_o$ ) ( $W/m^2K$ ), Winter 1997-1998  
(measuring accuracy =  $\pm 0.01 W/[m^2K]$ )**

Roof Type		Northeast	Southwest	Intended value
<b>Type 1: Compact</b>				
Variant with PE-foil	M	0.17	0.19	<b>0.18</b>
Variant without PE-foleE	M	0.17	<b>0.21</b>	<b>0.18</b>
	R	<b>0.16</b>	0.18	
<b>Type 2: Ventilated</b>				
Variant with PE-foil	M	0.18	<b>0.21</b>	<b>0.18</b>
Variant without PE-foleE	M	0.17	<b>0.19</b>	<b>0.18</b>
	R	<b>0.19</b>	<b>0.22</b>	<b>0.18</b>
	R	0.18	<b>0.28</b>	
<b>Type 3: Insulating underroof</b>	M	0.16	0.15	<b>0.16</b>
<b>Type 4: Sandwich</b>	M	0.24	0.22	<b>0.23</b>

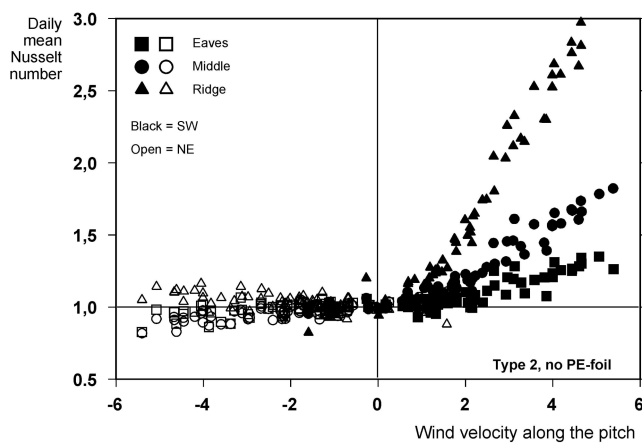


**Figure 7** Roof type 2, ventilated cathedral ceiling without polyethylene airflow and vapor retarder: measured Nusselt numbers as a function of the daily mean wind velocity component along the pitch. Reference thermal resistance at very low wind velocity:  $4.9 \text{ à } 5.4 \text{ m}^2K/W$ .

As the wind is blowing most of the time to the southwest, the vector is almost always positive along the southwest pitch and negative along the northeast pitch. Its impact on the local heat losses in fact depended on the orientation of the pitch and the distance from the eaves. At the windward side, losses increased from the eaves to the ridge, indicating that wind washing effects were strongest close to the ridge.

Table 3 summarizes the results for the compact and the ventilated cathedral ceiling types 1 and 2 by giving the reference clear roof U-factor and the Nusselt number at a wind velocity of 4 m/s. The reference fits closely with the intended value. The small differences noted are mainly a consequence

of the uncertainties with respect to the actual thickness of the glass-wool insulation. At the same time, the U-factor of the designs with a polyethylene airflow retarder hardly shows any influence of wind washing, while the U-factors of those without experience quite a few washing effects. On average, the two compact designs perform better than the two ventilated designs. In fact, the compact designs show a regain at the leeward side and less extra losses at the windward side.

An explanation of the wind velocity effects on the measured clear roof U-factor should be sought in the airflow patterns, revealed by the tracer gas measurements. At the windward side, wind pressure forces the outside air through the overlaps between the underlay lanes and washes the insulation below. As the flow resistance between windward and leeward side is smallest at the ridge, the largest effect is noted there. In the ventilated cathedral ceilings, the airspace with an air inlet and outlet between the underlay and the thermal insulation facilitates such wind washing. The heat regain effects noted in the two compact and two ventilated designs at the leeward side are linkable to air that warmed up while passing the insulation at the windward side, then flowed over the ridge to the upper parts of the insulation at the leeward side and moderated the heat loss there. Regain is less in the two ventilated designs, as the air crossing the ridge is easily dissipated into the airspace. The presence of a polyethylene airflow retarder protects the 5 cm of thermal insulation below it from wind-washing, resulting in a minor wind effect on the measured clear roof U-factor in the two compact and ventilated cathedral ceiling designs with such a retarder.

Globally, these results suggest that wind-tightness of the underlay should be a prime performance requirement in compact and ventilated cathedral ceiling roofs. That statement was confirmed through a series of additional clear roof U-factor measurements on the compact type 1 cathedral ceiling

**Table 3. Impact of Wind on the Measured U-Factor in the Two Traditional Cathedral Ceiling Types**

Roof Type		Northeast		Southwest	
		$U_0$ (W/(m <sup>2</sup> K))	Nu ( $v_{SW} = 4m/s$ )	$U_0$ (W/(m <sup>2</sup> K))	Nu ( $v_{SW} = 4m/s$ )
<b>Type 1: Compact</b>					
Variant with PE-foil	M	0.17	1.02	0.19	0.92
Variant without PE-folieE		0.18	0.73	0.19	1.28
	M	0.18	0.73	0.20	1.37
	R	0.17	0.75	0.16	1.59
<b>Type 2: Ventilated</b>					
Variant with PE-foil	M	0.18	0.99	<b>0.21</b>	1.06
Variant without PE-folieE		0.18	0.95	0.18	1.22
	M	0.20	0.92	0.19	1.55
	R	0.18	1.06	0.19	2.52

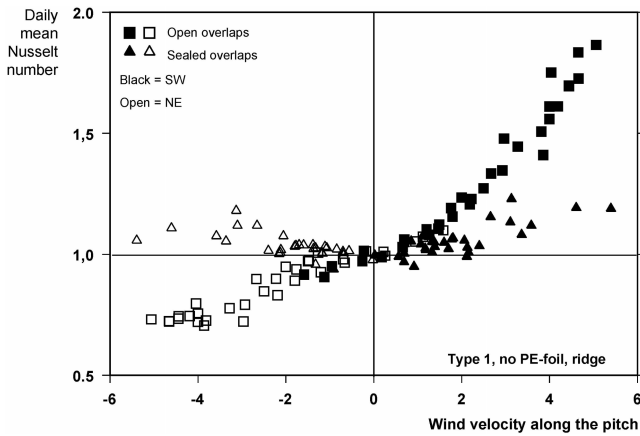


**Figure 8** Roof type 1, compact cathedral ceiling without polyethylene airflow and vapor retarder: measured Nusselt numbers as a function of the daily mean wind velocity component along the pitch, open and sealed underlay overlaps. Reference thermal resistance at very low wind velocity: 5.6 à 6.0 m<sup>2</sup>K/W.

without polyethylene foil after the overlaps between the underlay lanes were taped. The Nusselt numbers at the ridge went down considerably (Figure 8). The Nusselt numbers in the middle of the span and the Nusselt numbers one meter above the edges, however, did not change. One of the reasons could have been the quite important air permeability of the vapor-permeable underlay ( $a = 1.9 \cdot 10^{-4} \text{ kg}/[\text{m}^2 \cdot \text{s} \cdot \text{Pa}^b]$ ).

The clear roof U-factors discussed need a correction to take into account the two-dimensional and three-dimensional effects induced by the rafters and the horizontal paths. Accompanying thermal bridging effects could not be measured but were calculated using an appropriate software package. The calculation results were then verified through a comparison between calculated inside surface temperatures and an infra-

red picture of the inside surface. The impact of those thermal bridges on the whole roof U-factor differed between cathedral ceiling types. In type 4, the sandwich element roof, the impact was zero. In type 3, a 10% increase compared to the clear roof U-factor was noted. In the compact and ventilated types 1 and 2, despite the 5-cm-thick insulation layer between the horizontal laths below the rafters, the whole roof U-factor increased 20% compared to the clear roof U-factor. If these 5 cm below and 14 cm between the rafters were exchanged for 19 cm between the rafters only, the thermal bridge effect added 23% to the clear roof U-factor, i.e., hardly different from the situation as it is now. That result is illustrated in Figure 9. Table 4 compares the whole roof U-factors of the four cathedral ceiling types. Only type 3, the one with a 6-cm-thick XPS-insulating under-roof gives a value that fulfills the performance requirements, i.e., a whole roof thermal transmittance  $\leq 0.2 \text{ W}/(\text{m}^2 \cdot \text{K})$ .

**Interstitial Condensation**

Interstitial condensation requires a humidity source inside or outside the cathedral ceiling. That may be the inside air, the outside air, or a wet layer in the roof. Such a wet layer was not present during the field tests, as all cathedral ceilings started from air-dry conditions. In such cases, condensation may develop each time the vapor pressure on the inside or the outside air surpasses the saturation pressures at an interface anywhere in the ceiling. Whether condensation will happen or not, of course, also depends on the magnitude of the vapor flow from the environment under consideration to the interface and the direction of the vapor flow that leaves the interface to the other environment. However, the difference between the vapor pressure in the environment considered ( $p$ ) and the saturation pressure in the interface under scrutiny ( $p_{sat,s}$ ) acts as a driving force. That difference is called the condensation potential (CP) between an environment and a interface.

$$CP = p - p_{sat}(\theta_s)(Pa) \tag{5}$$

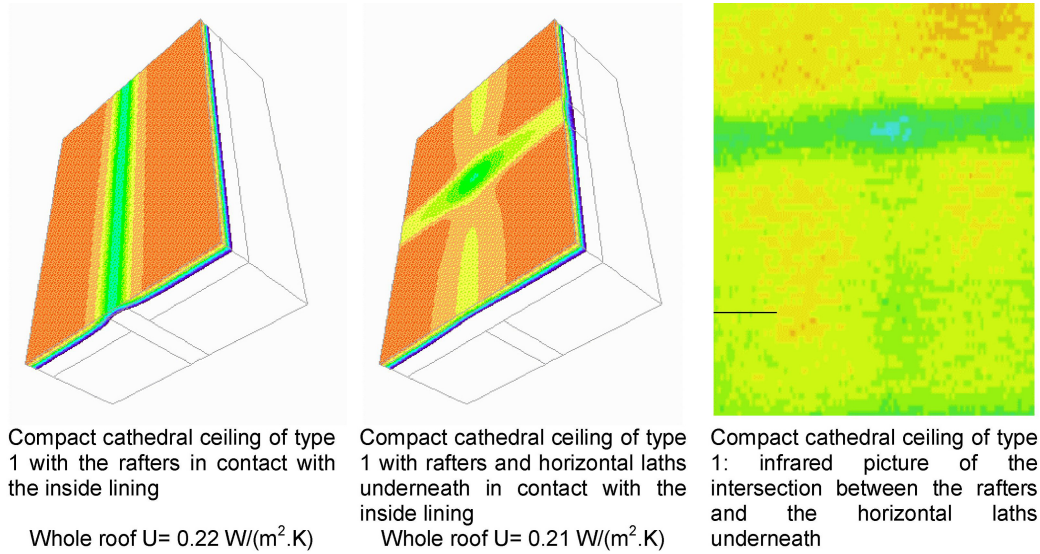


**Figure 9** Compact cathedral ceiling type 1 and ventilated cathedral ceiling type 2: a comparison between the calculated temperatures on the inside lining and the infrared image of the lining.

**Table 4. Whole Roof Thermal Performance (U)**

Roof Type	$U_0$ W/(m <sup>2</sup> ·K)	$\Delta U$ (wind effect, $v=4 \text{ m/s}$ ) W/(m <sup>2</sup> ·K)	$\Delta U$ Thermal bridging W/(m <sup>2</sup> ·K)	$U_{WR}$ W/(m <sup>2</sup> ·K)
Type 1: Compact	0.18	0.024	0.036	0.24
Type 2: Ventiladed	0.18	0.064	0.036	0.28
Type 3: Insulating under-roof	0.165	0	0.005	0.17
Type 4: Sandwich	0.23	0	0	0.23

If  $CP$  is positive, then the humidity in the environment considered may act as a condensation source for the interface. If negative, drying should occur. As the saturation pressure in an interface depends on the temperature of that interface, the outside air may act as a condensation source only if, as a result of clear sky longwave radiant cooling, the interface temperature drops below the outside dew-point temperature. As said, the inside air was kept on indoor climate class 3 conditions, which are representative for subsidized housing.

Table 5 lists the measured data for the cathedral ceiling type 3, for the compact cathedral ceiling type 1, and for the ventilated cathedral type 2, the last two for the designs with polyethylene airflow retarder. The total time that a zero value for undercooling and for the daily mean condensation potential was exceeded, together with the 10% and 90% percentiles, is given. Averaged over the winter months, the surface temperature of the tiles and the underlay was lower than the outside air temperature. On all northeast-oriented pitches, the tiles were undercooled during one-third of the time over the whole testing period and the underlay during one-fourth of the time.

Thanks to the sun, lower percentages were experienced on the southwest-oriented pitches. Despite the large number of undercooling days, the condensation potential for the outside air remained negative, or the outside air acted, on average, as a drying medium over the whole test period. The inside air on the contrary figured as a potential condensation source during half of the period. In the northeast, the condensation potential ( $CP_i$ ) remained positive from October until April; in the southeast, it remained positive from November until March ( $CP_i = 300 \text{ à } 600 \text{ Pa}$ ). Altogether, the differences between the compact type 1 and the ventilated type 2 cathedral ceiling remained very small, with some advantage for the compact type 1 in summer, when the drying potential scored higher than in the ventilated type 2. The use of an insulating XPS underroof in type 3 resulted in a substantial difference. There, the temperature at the underside of the XPS remained high enough to prevent the inside air humidity from becoming a potential condensation source except for a couple of days in early November 1997.

**Table 5. Statistical Distribution of the Daily Mean Values for Undercooling and Condensation Potential Related to the Roof Cover and the Underlay. (433 days from 8/1/1997 to 30/6/1998)**

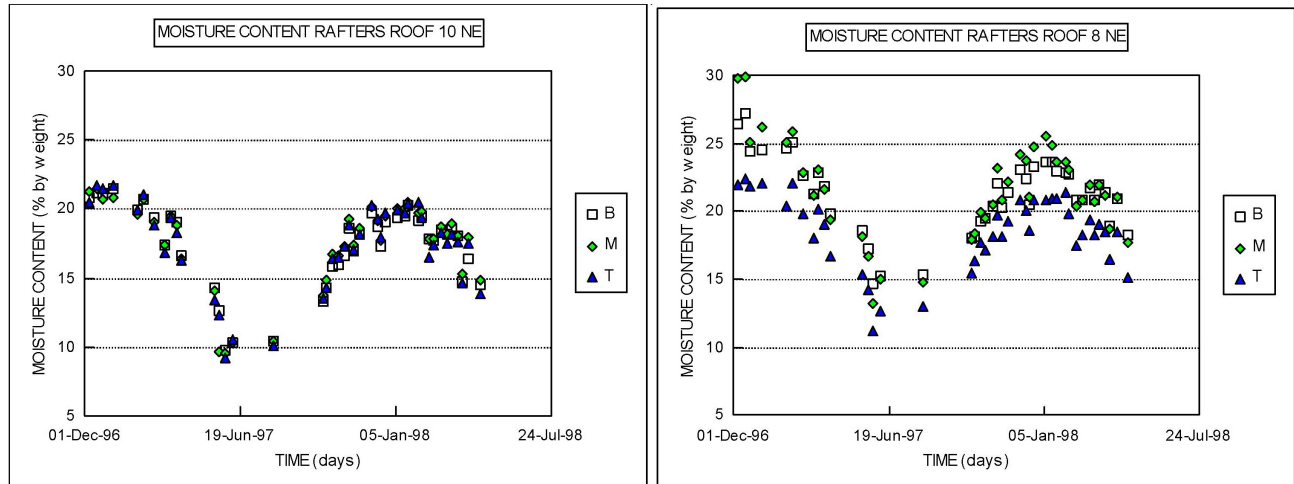
Roof Type		UNDERCOOLING $\theta_s - \theta_e$ (°C)			CP OUTSIDE AIR $p_e - p_{sat}(\theta_s)$ (hPa)			CP INSIDE AIR $p_i - p_{sat}(\theta_s)$ (hPa)		
		<0	10%	90%	>0	10%	90%	>0	10%	90%
<b>Type 1: Compact Variant with PE-Foil</b>										
NORTHEAST	tile	37%	-1.7	4.4	4%	-13.6	-0.5	50%	-13.1	5.0
Underlay	E	26%	-1.0	4.7	1%	-14.0	-1.0	46%	-13.3	4.5
Underlay	M	24%	-0.9	5.4	0%	-15.2	-1.0	45%	-14.3	4.5
Underlay	R	17%	-0.5	5.8	0%	-16.4	-1.2	43%	-15.6	4.5
SOUTHEAST, underlay	M	8%	0.3	7.2	0%	-17.2	-1.5	39%	-16.2	3.7
Underlay	R	9%	0.1	8.0	0%	-18.8	-1.4	40%	-17.8	3.8
<b>Type 2: Ventilated Variant with PE-Foil</b>										
NORTHEAST	tile	34%	-1.7	4.9	2%	-14.6	-0.6	48%	-13.6	4.8
Underlay	E	24%	-0.7	3.1	0%	-10.6	-1.0	47%	-10.3	4.5
Underlay	M	28%	-0.9	3.9	0%	-12.7	-0.9	47%	-12.3	4.7
Underlay	R	18%	-0.5	5.1	0%	-14.9	-1.2	44%	-13.7	4.3
SOUTHEAST, underlay	E	12%	-0.1	3.9	0%	-10.9	-1.3	46%	-9.8	4.0
Underlay	M	11%	-0.1	4.3	0%	-11.4	-1.4	46%	-10.3	3.9
Underlay	R	16%	-0.3	5.6	0%	-13.9	-1.2	44%	-12.9	4.0
<b>Type 3: Insulating under-roof</b>										
NORTHEAST	XPS	0%	3.7	8.5	0%	-13.3	-6.7	1%	-12.5	-1.5

Of course, a positive condensation potential does not mean that condensate will be deposited. Whether or not that happens depends on the overall air permeability of the roof and the vapor resistances at both sides of the interface considered in the roof. To get information on the actual condensation deposit, condensation sensors were used in both the compact type 1 and ventilated type 2 cathedral ceilings. These sensors produce a peak in electrical current each time water droplets are deposited on the conductors of the active matrix of the sensor. There is a signal when condensation starts and stops, but no information on quantities is given. Table 6 summarizes the number of days during which peaks in electrical current were registered. In the four cathedral ceiling types, these peaks were very temporary. On the day of their appearance, the signal fell back below the threshold of detection, indicating that condensation was a transient phenomenon between day and night. The number of days that peaks were noted was generally very limited, especially if one takes into account that the outside air humidity could also act as a momentary moisture source. Apparently, the moisture control strategies employed in the two cathedral ceiling types 1 and 2 worked well (airflow retarder and some vapor retarding quality on the inside in combination with ventilation or a vapor permeable underlay).

Nevertheless, there were differences between the roofs. The ventilated roof type 2 without polyethylene foil suffered the most from condensation at 1 m from the eave in the southwest-oriented pitches. The peaks at that spot are most probably linked to the inflow of ventilation air at moments that the underlay is undercooled. Yet, in the compact roof type 1 without polyethylene foil, the number of condensation days in the southwest pitch was very low. Most condensation days were recorded in the northeast pitch, 1 m from the ridge. This is probably a consequence of tiny air leaks at the intersection of the inside lining and the ridge rafter, causing inside air to infiltrate into the northeast-oriented pitch. The number of condensation days in the compact type 1 and ventilated type 2 with polyethylene foil was only one-third of the value measured in the compact type 1 and ventilated type 2 without polyethylene foil. The polyethylene foil also annihilated the difference between compact and ventilated.

### Sorption Moisture in the Rafters

The moisture content in the central rafter of the compact roof type 1 and the ventilated roof type 2 was measured weekly just below the underlay, using an electrical resistance meter. Independent of the presence of a polyethylene airflow retarder,



**Compact cathedral ceiling of type 1 with poly-ethylene airflow and vapor retarder**      **Ventilated cathedral ceiling of type 2 with polyethylene airflow and vapor retarder**

**Figure 10** Measured moisture content in the rafters, just below the underlay, in the compact cathedral ceiling type 1 and the ventilated cathedral ceiling type 2.

**Table 6. Days with Condensation Between 8/1/1997 and 30/6/1998**

Roof Type		Northeast	Southwest
<b>Type 1: Compact</b> Variant without PE-foil	E		5 (1%)
	M	15 (3%)	14 (3%)
	R	25 (6%)	
<b>Type 1: Compact</b> Variant with PE-foil	E		4 (1%)
	M	-	5 (1%)
	R	6 (1%)	
<b>Type 2: Ventilated</b> Variant without PE-foil	E		47 (11%)
	M	13 (3%)	9 (2%)
	R	-	
<b>Type 2: Ventilated</b> Variant with PE-foil	E		17* (4%*)
	M	7 (2%)	7 (2%)
	R	5 (1%)	

\* Extrapolated, starting from incomplete data (8/1/1997-7/11/1997)

the evolution in sorption moisture hardly differed between the two roof types: a seasonal fluctuation with the highest values at the end of the winter and the lowest at the end of the summer (Figure 10). The relative humidity below the underlay showed an analogous fluctuation. In the ventilated roof type 2, moisture content also decreased from eave to ridge, while in the compact type 1, moisture content was quite constant, independent of the position along the span. Mold risk at mid-span on the central rafter in the compact roof type 1 and the ventilated roof type 2 is shown in Figure 11 for the northeast-oriented pitches.

Although the ventilated roof type 2 does not satisfy the criterion of a moisture ratio permanently lower than 20% kg/kg, the measured values of moisture ratio and temperature hardly entered the zone of mold risk larger than 5%. Application of a protective treatment should therefore be sufficient to eliminate any risk.

## CONCLUSIONS

The field tests on the six cathedral ceilings generated the following conclusions:

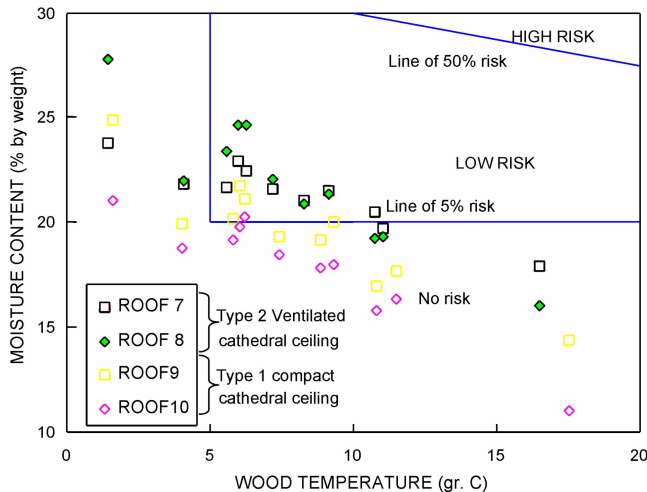


**Figure 11** Mold attack risk upside the rafters, based on the measured temperature and moisture ratio (monthly mean values). Roofs 7 and 8 stand for the ventilated cathedral ceiling type 2, roofs 9 and 10 for the compact cathedral ceiling type 1. Roofs 8 and 10 are the designs with polyethylene airflow and vapor retarder).

- A sufficient airtightness of the inside lining eliminates the inside humidity as a parameter that may impact the moisture response of a compact (type 1) and a ventilated (type 2) cathedral ceiling. The tests show that a surface-averaged permeance coefficient of  $7.2 \cdot 10^{-6} \text{ kg}/(\text{m}^2 \cdot \text{s} \cdot \text{Pa}^b)$  is largely sufficient for that. That value is in close agreement with the threshold of  $1 \cdot 10^{-5} \text{ kg}/(\text{m}^2 \cdot \text{s} \cdot \text{Pa}^b)$ , found as performance requirement for metallic roofs in cool climates (Hens et al. 2003).
- The fact that the polyethylene airflow and vapor retarder hardly has any impact on the condensation deposit at the backside of the underlay and the sorption moisture built up in the rafters underlines that diffusion from moisture generated inside is a minor factor once a sufficient airtightness is guaranteed. What is left is a moisture response, mainly influenced by the exterior climate (relative humidity, undercooling, solar irradiation, rain). The more outside air ingresses into the cathedral ceiling, which is the case in the ventilated roof type 2, the more explicit that influence is. The combination of undercooling, high outside relative humidity, and a very limited solar irradiation, which is the case in the northeast, may invoke quite a few condensation peaks at the backside of the underlay and result in much hygroscopic moisture in the top layer of the rafters during wintertime.
- Wind washing has an important impact on the thermal performance of a compact and a ventilated cathedral ceiling in cool climates. How important this is depends

on pitch orientation, type of cathedral ceiling, and position of the airflow and vapor retarder. A leeward orientation is less vulnerable than a windward orientation. A compact cathedral ceiling performs better than a ventilated cathedral ceiling (although that advantage disappears in case the insulation is too lightweight), and positioning part of the thermal insulation between an airflow and vapor-retarding foil and the internal lining is a benefit. Underlay foils with open overlaps between lanes, whether vapor-permeable or not, are a disadvantage that should not be used.

Overall, the compact roof type 1 performed better than the ventilated roof type 2. The differences, however, are minimal in case sufficient airtightness below the insulation is realized. The type 3 cathedral ceiling with insulating underroof proved to be an excellent choice. It was sufficiently airtight, hardly suffered from wind-washing, had a constant clear roof thermal transmittance over time, showed minimal thermal bridging, and neither suffered from interstitial condensation nor from problematic sorption moisture content in the rafters. The type 4 cathedral ceiling also performed well. The only drawback was the usage of a too lightweight EPS as sandwich fill, resulting in a clear roof thermal transmittance that did not comply with the whole roof requirement of  $0.2 \text{ W}/(\text{m}^2 \cdot \text{K})$ .

The two years of field testing allowed the consortium to refine the construction rules for cathedral ceilings with high thermal performance (whole roof U-factor  $\leq 0.2 \text{ W}/[\text{m}^2 \cdot \text{K}]$ ).

1. Use a sufficiently dense but flexible thermal insulation with thickness  $\geq 20 \text{ cm}$ . Fill the whole height of the rafters without leaving an airspace between underlay and insulation.
2. Care for a continuous airflow retarder at the inside of the insulation, with all joints taped and all contact lines sealed between foil and walls, foil and windows, foil and beams.
3. Provide a wiring cavity at the inside of the airflow retarder. Fill that cavity with insulation once the wiring is finished.
4. Use a wind-tight, vapor-permeable underlay (vapor permeance close to  $1 \cdot 10^{-10} \text{ s}/\text{m}$ ) with sealed overlaps between the lanes.
5. Detail eaves and ridge so that wind-tightness is guaranteed.

## ACKNOWLEDGMENT

We would like to thank the Flemish Government and the European Roof Industry for their financial support.

## REFERENCES

- Anon. 1975-2000. Reports on sloped roof damage cases, K.U.Leuven, Laboratory of Building Physics (in Dutch, not public domain).
- Anon. 1982. Vochtgedrag van bouwdeelen (Moisture response of building elements), special issue of the WTCB-tijdschrift, Vol. 17, March.
- Anon. 1989. The Redland Roofing Manual, 2d ed., Redland Roof Tiles Ltd.

- ASTM. 1995. ASTM C1155, Standard practice for determining thermal resistance of building envelope components from in-situ data. Annual book of ASTM standards. ASTM, Pa. 1998.
- BIN/IBN. 1987. Calculation of the thermal transmittance of walls in buildings, NBN B 62-002 (in Dutch and in French).
- Derome, D. 1998. Testing of flat roof insulated with cellulose fiber. *Proceedings of the Thermal Performance of the Exterior Envelopes of Buildings VII, Clearwater Beach*, pp. 3-13.
- Hendriks, L., and H. Hens. 2000. Building envelopes in a holistic perspective, Final Report IEA, EXCO ECBCS, Annex 23 IBEPa, p. 101 & addenda.
- Hens, H., and A. Janssens. 1999. Heat and moisture response of vented and compact cathedral ceilings: A test house evaluation. *ASHRAE Transactions* 105(1):837-850.
- Hens H., R. Zheng, and A. Janssens. 2003. Does performance based design impacts traditional solutions? Metal roofs as an example. *Research in Building Physics*, Balkema, pp. 557-564.
- Janssens A., H. Hens, A. Silberstein, and J. Boulant. 1992. The influence of underroof systems on the hygrothermal performance of sloped insulated roofs. *Proceedings of the Thermal Performance of the Exterior Envelopes of Buildings V, Clearwater Beach*, Dec. 7-10, Vol. 1, pp. 368-378.
- Janssens A., H. Hens en, and S. Roels. 1995. VLIET test building, Laboratorium Bouwfysica, K.U.Leuven (in Dutch).
- Janssens, A., and H. Hens. 1998. Final report contract IWT/VLIET/930235. Laboratory of Building Physics. K.U.Leuven (in Dutch).
- Janssens, A., W. Depraetere, and H. Hens. 1999. Impact of air infiltration on the performances of highly insulated walls and roofs. *Bouwfysica tijdschrift* 99(4):22-28 (in Dutch).
- Janssens, A., and H. Hens. 1999. Thermal effects of wind-washing in duo-pitched tiled roofs. *Proceedings of the 5th symposium of Building Physics in the Nordic Countries, Goteborg, Sweden*, pp. 417-424.
- Künzel, H., and Th Großkinsky. 1989. Untersuchungen über die Feuchteverhältnisse bei wärmegeämmten Satteldachkonstruktionen, FB-25/1989 Fraunhofer-Institut für Bauphysik, Holzkirchen (in German).
- Künzel, H., and Th Großkinsky. 1992. Vorteile diffusionsoffener, unbelüfteter Satteldachkonstruktionen, FB-39/1992 Fraunhofer-Institut für Bauphysik, Holzkirchen (in German).
- Ojanen, T. 2001. Thermal and moisture performance of a sealed cold roof system with a vapor-permeable underlay. *Proceedings of the Thermal Performance of the Exterior Envelopes of Buildings VIII, Clearwater Beach*, Dec. 3-6 (CD-ROM).
- Rose, W.B. 2001. Measured summer values of sheathing and shingle temperatures for residential attics and cathedral ceilings. *Proceedings of the Thermal Performance of the Exterior Envelopes of Buildings VIII, Clearwater Beach*, Dec. 3-6 (CD-ROM).
- Sanders, C. 1996. Environmental conditions, Final report, Annex 24 Hamtie, Task 2, ACCO, pp. 96.
- Sedlbauer, K., and H.K. Künzel. 2000. Field tests confirm the trend: Vapour-permeable is better than vapour-tight. *Proceedings of the International Building Physics Conference, Eindhoven*, pp. 555-563.